

Understanding EC-EARTH winter mean precipitation over the tropical Pacific: implications for prediction skill.

Author: Rubèn Burillo Martí

Supervisors: Javier García Serrano, j.garcia-serrano@meteo.ub.edu and Yolanda Sola, ysola@meteo.ub.edu
*Facultat de Física, Universitat de Barcelona, Diagonal 645, 08028 Barcelona, Spain.**

Abstract: This study investigates the seasonal variability of convective precipitation (cPCP) and stratiform precipitation (sPCP) in the tropical Pacific, using hindcasts from the European Community Earth System model (EC-EARTH). Our analysis revealed that cPCP is primarily driven by sea surface temperature (SST), with warmer SSTs leading to increased convective activity. In contrast, thanks to its correlation with SST and also surface solar radiation downwards, results indicate sPCP is more influenced by atmospheric processes. sPCP and cPCP correlation is positive throughout all the tropical Pacific region although, their correlation is negative in the eastern Intertropical Convergence Zone (ITCZ). This region has been studied in detail considering the correlation between the different types of precipitation and the surface latent heat flux (LHF). It has been concluded that in the eastern ITCZ, LHF contributes to increase cPCP rather than sPCP, explaining the negative correlation between them. The study also highlights the limitation of observational data, which usually only provides total precipitation, thereby restraining the ability of the model to predict each precipitation component accurately. Our findings emphasise the possibility for separating precipitation data into cPCP and sPCP to improve model skill by computing the potential predictability of both components.

I. INTRODUCTION

Precipitation (PCP) is usually separated in atmospheric models into stratiform and convective components. The European Community Earth System model (EC-EARTH) parametrises convective processes using a mass-flux scheme which determines the convective updrafts and downdrafts while large-scale processes that involve stratiform precipitation are resolved using detailed prognostic equations (ECMWF 2016). However, when it comes to observations, this separation is not always possible. Some precipitation events are not purely convective or purely large-scale but exhibit characteristics of both, so reanalysis data usually only provide total precipitation (Tapiador 2012). To assess prediction skill, model outputs are compared to observations to evaluate model performance. If observed PCP is not divided into convective (cPCP) and stratiform (sPCP) components, model precipitation skill must rely on total precipitation. Thereby, the potential benefits of distinguishing between the two precipitation types are lost. For instance, the inability to separate observed precipitation does not allow us to evaluate the model capability to predict each component and translate it into prediction skill.

Previous research has evaluated model precipitation skill by examining its correlation with total precipitation observations. Additionally, when assessing precipitation skill on a seasonal timescale, correlation between PCP and sea surface temperature (SST) is also considered, due to the impact SST has on PCP (Arakawa and Kitoh 2004; Chen et al. 2012). The slowly-varying sea

surface conditions and their influence on the atmosphere provide seasonal predictability to PCP, thus, frequently those regions where model seasonal PCP skill is high do also exhibit a high SST-PCP correlation. In contrast, atmosphere dynamics have a much faster variability which counters this ocean long-lasting precipitation forcing. Therefore, to understand the geographical variations in the SST-PCP correlations and their amplitude, PCP variability must be divided into two possible mechanisms: sea driven and atmosphere driven. In both mechanisms, PCP and SST variability are connected to surface solar radiation downwards (SSRD), since changes in PCP affect downward solar radiation and, consequently, end up modifying ocean surface conditions (Kumar et al. 2013). Therefore, SSRD must be considered in both oceanic and atmospheric mechanisms. The following schemes for PCP variability are considered throughout this study:

$$Sea - driven : \uparrow SST \Rightarrow \uparrow PCP \Rightarrow \downarrow SSRD$$

$$Atm - driven : \uparrow PCP \Rightarrow \downarrow SSRD \Rightarrow \downarrow SST$$

In the Sea-driven mechanism, SST anomalies are considered first. Changes in SST modify the surface evaporation rate, consequently altering the water vapour content in the atmosphere. If SST increases (decreases), the surface evaporation rate is enhanced (reduced). An increase (decrease) in water vapour concentration contributes to enhanced (reduced) cloud formation and therefore an increase (decrease) in PCP (Waliser and Graham 1993). Moreover, water vapour molecules can undergo various vibrational and rotational transitions when exposed to solar radiation at specific wavelengths, absorbing part of it. Apart from this absorption, solar radiation can also be partially reflected by clouds

* Electronic address: rburillo17@gmail.com

due to their high albedo (Wallace and Hobbs 2006). Consequently, the PCP anomalies induced by SST do also affect SSRD. In this Sea-driven mechanism, SST-PCP correlation is positive and PCP-SSRD correlation is negative. On the other hand, in the Atm-driven mechanism, PCP anomalies are considered first. These anomalies can be caused by moist (dry) advections that increase (decrease) the specific humidity and upwards (downwards) movements that increase (decrease) water vapour condensation and enhance (reduce) cloud formation (Holloway and Neelin 2009). Considering the same processes as in the Sea-driven mechanism, due to these PCP anomalies, SSRD decreases (increases). This changes in solar radiation reaching the surface leads to a decrease (increase) in SST. In this Atm-driven mechanism, SST-PCP correlation is negative as well as PCP-SSRD correlation. However, these variability schemes for PCP and the role SSRD plays in them are very simple. Kumar et al. (2013) suggested that to understand better how PCP seasonal variability works and how it is translated into model seasonal prediction skill, it is necessary to study in detail SSRD and other surface fluxes, such as latent heat flux (LHF).

When studying seasonal variability, the tropical Pacific is a particularly important region to consider. This region is significantly influenced by the El Niño-Southern Oscillation (ENSO), which has a substantial impact on global climate patterns. ENSO is a coupled climate phenomenon with an oceanic and atmospheric component. Its ocean variability consists of an SST oscillation with a characteristic period of 2 to 7 years, occurring in the central-eastern equatorial Pacific. Positive (negative) SST anomalies are referred to as El Niño (La Niña). SST anomalies start in early boreal summer, develop over the equatorial Pacific, and peak in boreal winter (DJF). This frequency and development of ENSO events contribute to its high seasonal predictability. The atmospheric variability of ENSO, known as the Southern Oscillation, is characterised by an interannual oscillation in tropical sea level pressure between the western and eastern tropical Pacific. This oscillation is influenced by the zonal SST gradient which is defined by a cold SST tongue along coasts of Peru and Chile in the eastern Pacific, and a warm SST pool across the Indo-Pacific region. This SST gradient affects the intensity of the easterly trade winds over the tropical Pacific (Wang and Picaut, 2004). At the same time, the trade winds also modify SST by reducing or enhancing evaporation and the upwelling of cold water. Bjerknes (1969) recognised this connection between both oceanic and atmospheric components and postulated a positive ocean-atmosphere feedback responsible for the development of ENSO events.

ENSO events trigger major changes in tropical PCP, especially in the tropical Pacific, since shifts in convection regions, such as the Indo-Pacific, occur depending

on the different phases of ENSO. They do also affect the Intertropical Convergence Zone (ITCZ), which is the region near the equator where the trade winds converge, leading to rising air, cloud formation, and strong precipitation (Xie 2004). The ITCZ main shifts are in response to the seasonal movement of the maximum solar radiation, which indicates that it is a region strongly involved with SSRD. However, the ITCZ is also enhanced by SST: Positive SST anomalies (El Niño phase) tend to draw the ITCZ towards them, while negative SST anomalies (La Niña phase) tend to shift it away.

Given the critical role of ENSO and the ITCZ in modulating atmospheric circulation patterns in the tropical Pacific, understanding these phenomena is essential for comprehending PCP variability. Studying their impacts on surface fluxes and their interaction with PCP provide valuable insights into seasonal PCP variability.

The primary objective of this study is to investigate the seasonal variability of precipitation (PCP) in the tropical Pacific. This investigation aims to enhance understanding of the mechanisms governing PCP variability in this region and their implications for global climate models. First, we consider separating PCP into cPCP and sPCP and study their climatologies. Afterwards, we assess which mechanisms are driving each type of PCP variability studying their correlation with SST first and SSRD after. Finally, we provide a more complex analysis by evaluating the correlations between PCP-LHF and SSRD-LHF. Two other surface fluxes and their correlation with PCP have also been studied: sensible heat flux (SHF) and surface thermal radiation upwards (STRU). However, since they did not provide relevant information for the work, only SSRD and LHF will be addressed. Through the analysis of SST, SSRD and LHF, we expect to be able to identify how seasonal variation patterns, like ENSO, affect surface fluxes and consequently how they may affect precipitation. Furthermore, understanding the mechanisms driving these changes in surface fluxes, and investigating their impact on PCP variability, can contribute to an improved understanding of the EC-EARTH model used in this analysis. Specifically, a detailed analysis of the results aims to enhance understanding of the model skill in simulating precipitation patterns and its possible implications.

II. DATA AND METHODOLOGY

A. Data sets

For the analysis of this study, outputs from the EC-EARTH model are used. The EC-EARTH model is a global climate model with coupled atmospheric and oceanic components. Its atmospheric component is the Integrated Forecast System (IFS, cycle 36r4)

of the ECMWF at T255 horizontal resolution which corresponds approximately to 60 km. Its oceanic component is the Nucleus for European Modelling of the Ocean (NEMO, version 3.3.1) at the nominal horizontal resolution ORCA1 which corresponds to approximately 110 km, coupled to the second version of the Louvain-la-Neuve (LIM2) sea ice model. Extended winter (NDJF) is the season chosen for the study since it is the season when ENSO anomalies are usually at their maximum and, therefore, its impact on the tropical Pacific is most pronounced. The data analysed are seasonal hindcasts initialised on the 1st of November each year over 1993 to 2009 and ending on the 28th/29th of February of the following year. The simulation for each winter has been initialised 10 times with slightly different initial conditions to sample the observational inaccuracy (Buizza 1999), resulting in a 10-member ensemble hindcast. More details on the model configuration and experimented setup can be found in Prodhomme et al. (2016) and Haarsma et al. (2019).

SST and PCP reanalysis have also been used as observations to compare with model data: the Hadley Centre Sea Ice and Sea Surface Temperature data set (HadISST) and the CPC Merged Analysis of Precipitation (CMAP). Data resolution is $1^\circ \times 1^\circ$ for HadISST and $2.5^\circ \times 2.5^\circ$ for CMAP. Since these resolutions are different from the model one, when computing the correlations between model data and these reanalysis, a linear interpolation is made to the model data so the resolutions are the same as the reanalysis.

B. Methodology

Each model variable studied has a particular mean state associated with the time period analysed known as climatology. Climatology is computed as the averaged value of each variable in each of the 10 members. The mean of the different model members is known as the ensemble mean. The reason to compute the ensemble mean is to retain the variability all members share and to eliminate the noise that each individual member has. Anomalies are considered deviations from the ensemble-mean climatology, and variability is estimated as the standard deviation of these anomalies.

To evaluate the relationship between the anomalies of different variables, their correlation coefficient is computed. Correlation value and sign indicate the strength and direction of the possible connection between them. We must point out that all correlations between different variables are point-to-point, that is, only their correlation at each grid point is assessed. However, possible teleconnections to ENSO are relevant to our study, and with point-to-point correlations we may not be able to assess them. Therefore we compute an index that can describe the variability of ENSO. To characterise ENSO with an index, the area-averaged value of SST anomalies in the

central-equatorial Pacific will be computed in the Niño-3.4 region (5°S – 5°N , 190° – 240°E) (Deser et al. 2010). This region is indicated in Fig 1. We call this index the Niño-3.4. Correlations between Niño-3.4 and any other variables indicate a possible teleconnection with ENSO. Furthermore, a correlation t-test, with null hypothesis of being zero, has been conducted to all correlations. Since the sample size is sufficiently large, it is considered to approximately follow a normal distribution, and therefore the t-test is valid to evaluate whether the observed correlations between variables are statistically significant.

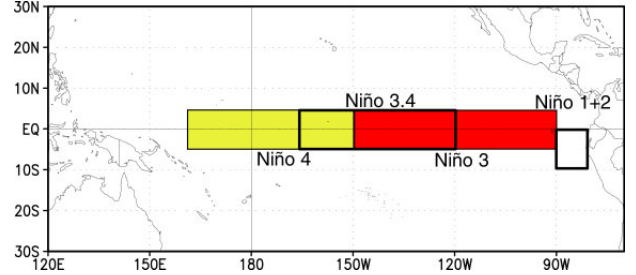


Figure 1. ENSO index regions from NOAA Climate Prediction Center.

Lastly, to assess the skill of the model, its predictions must be compared with observational data. As mentioned earlier, reanalysis only provide total precipitation data so the sum of model convective and stratiform precipitation is considered as the model total precipitation. Model skill is evaluated with the correlation coefficient between this total precipitation and the reanalysis precipitation. Although this comparison is the best way to assess the capability of the model for prediction, it is important to note that the analysed model data consists of a 10-member ensemble of hindcasts. This ensemble allows us to evaluate the model potential predictability. Potential predictability is the ratio of variance that the model is capable to consistently predict in its reality, which might well be different from that in nature. It is computed as the fraction between the ensemble mean variance and the total variance, which includes both the predictable variance and the unpredictable noise variance.

III. RESULTS

Model PCP data is separated into cPCP and sPCP. To better understand their variability and their correlation with the other variables, we start evaluating their climatologies, which are presented in Figs 2a and 2b respectively. Comparing both figures, convective precipitation dominates over all the tropical Pacific. In cPCP climatology, a wide region with high precipitation is observed in the Indo-Pacific region, which is known for high SST, enough to trigger atmospheric deep convection (Johnson and Xie, 2010). In the central Pacific, two strips of precipitation are observed: the ITCZ in the

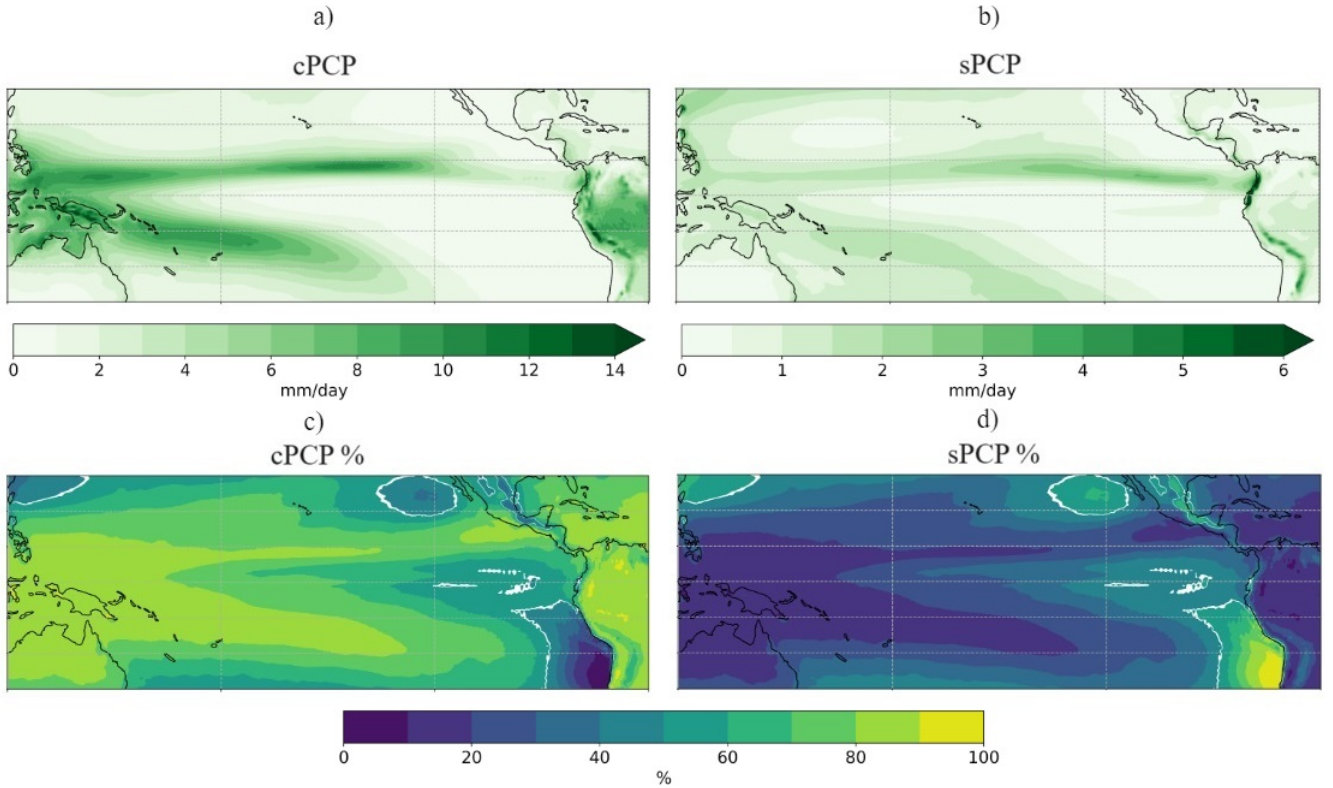


Figure 2. a) and b): NDJF climatology of model cPCP and sPCP. Both PCP units are mm/day. c) and d): NDJF model cPCP and sPCP climatology percentage within the climatology of total precipitation. Total precipitation is considered as the sum of cPCP and sPCP. White lines represent the 50% value.

equatorial region and the Southern Pacific Convergence Zone (SPCZ) further south. Also, a significant precipitation region is found in cPCP climatology in the Amazon basin, along with a band in the western South America, which is the precipitation occurring along the Andes. The same precipitation patterns are present in sPCP climatology but with a weaker amplitude compared to cPCP. However, looking at both climatologies, we observe a division in the ITCZ into two sections: a convective part in the western-central region, and a stratiform part in the eastern region. To visualise this more clearly, the percentages of cPCP and sPCP relative to total precipitation, which is the sum of both, are shown in Figs 2c and 2d respectively. We observe that in the western-central ITCZ, cPCP is dominant, while in the eastern ITCZ both cPCP and sPCP have a similar contribution to total precipitation.

Next, we explore the correlation of cPCP and sPCP with SST, since oceanic conditions play a major role in tropical Pacific precipitation variability. By analysing how cPCP and sPCP respond to variations in SST we are able to assess if PCP is either Sea-driven (positive SST-PCP correlation) or Atm-driven (negative SST-PCP correlation). The correlation coefficients between SST-cPCP and SST-sPCP are shown in Figs

3a and 3b respectively. Convective precipitation has a positive correlation with SST throughout the equatorial Pacific, suggesting a significant influence of SST in convective patterns. The regions that exhibit the strongest SST-cPCP correlations include the ITCZ and the SPCZ, whereas no significant correlation is observed in the SST cold tongue along the coasts of Peru and Chile, as well as in the northern central Pacific above the ITCZ. Stratiform precipitation exhibits a similar positive correlation pattern with SST along the equator, although weaker in the western Pacific. In the eastern ITCZ though, there is a negative SST-sPCP correlation indicating that, unlike other regions, stratiform precipitation in this area could be Atm-driven. The PCP mechanisms considered also involve SSRD, so the SST-SSRD correlation map (Fig 3c) can be useful to clarify if sPCP is Atm-driven. First of all, in the western and central Pacific, correlation is negative, with the ITCZ exhibiting the strongest negative correlation, indicating that this region is mainly Sea-driven. Conversely, in the eastern ITCZ, the SST-SSRD correlation is positive, confirming that at least sPCP in this region is primarily driven by atmospheric processes. However, as mentioned earlier, SST-cPCP shows a positive correlation (Fig. 3a), indicating that convective precipitation in this area is also influenced significantly by SST.

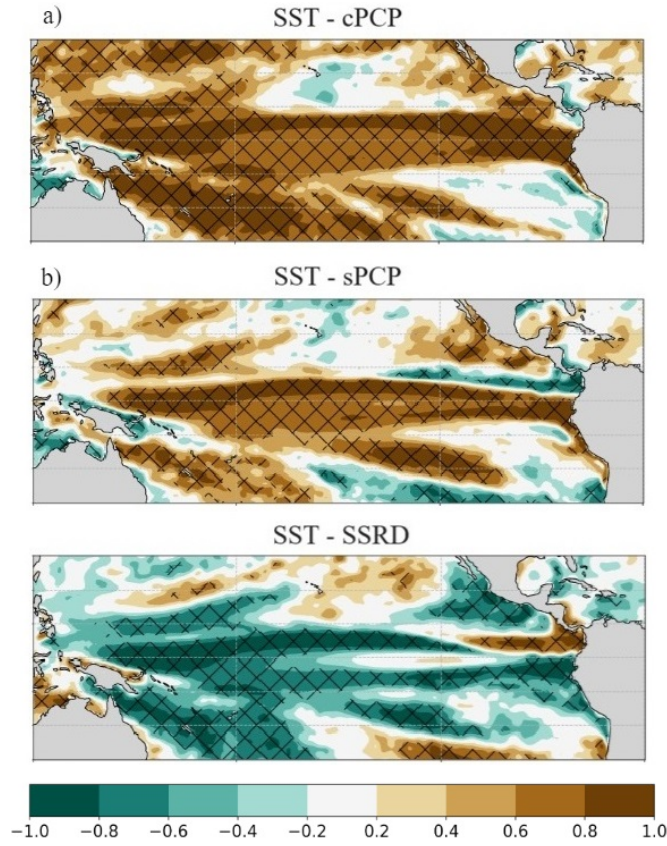


Figure 3. a), b) and c): Correlation coefficient between model SST and model cPCP, sPCP and SSRD respectively. SSRD flux is defined positive downwards. Statistically significant regions at 95% confidence level are hatched.

With this first analysis, we observe that throughout the tropical Pacific, PCP is strongly influenced by oceanic variability rather than atmospheric variability. However, in the eastern ITCZ, cPCP and sPCP exhibit a different behaviour compared to the PCP in the western-central ITCZ. In the eastern ITCZ section, SST-sPCP correlation is negative, while SST-cPCP correlation is positive, suggesting that sPCP is controlled by an Atm-driven mechanism and cPCP by a Sea-driven mechanism. However, the positive SST-SSRD correlation indicates that an Atm-driven mechanism might be occurring in the eastern ITCZ. To further understand this, we can examine the correlation maps between SSRD-cPCP and SSRD-sPCP presented in Figs 4a and 4b respectively. For both PCP variability mechanisms considered, PCP-SSRD correlation is negative, since changes in cloudiness due to precipitation and SSRD tend to be opposite. This negative correlation is observed overall in both SSRD-cPCP and SSRD-sPCP correlation maps all across the tropical Pacific. However, a significant SSRD-cPCP positive correlation appears in the eastern ITCZ. A positive correlation between SSRD and PCP was not considered

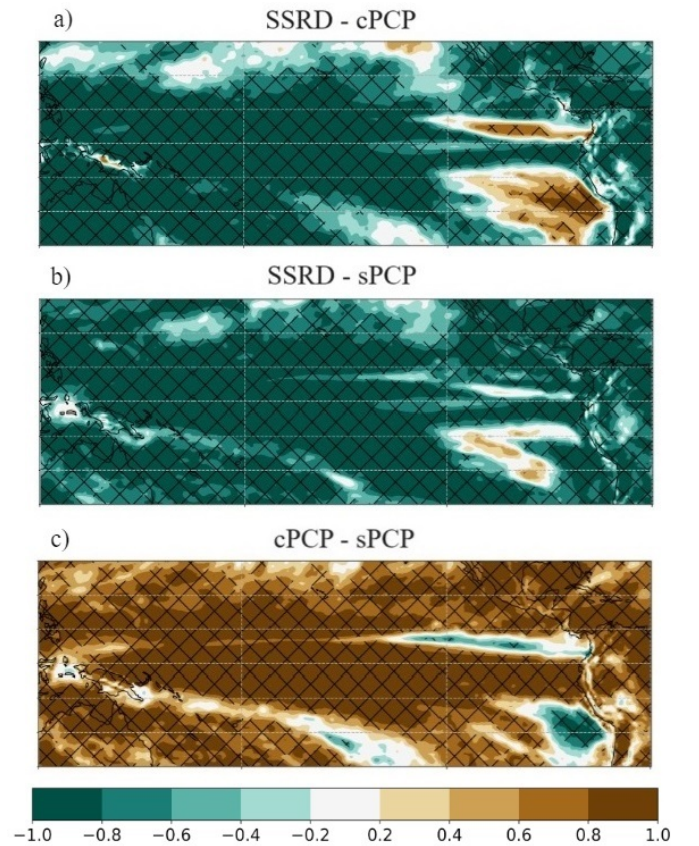


Figure 4. a) and b): Correlation coefficient between model SSRD and model cPCP and sPCP respectively. SSRD flux is defined positive downwards. c): Correlation coefficient between model cPCP and sPCP. Statistically significant regions at 95% confidence level are hatched.

in either the Sea-driven or the Atm-driven mechanisms, therefore these mechanisms might not be able to describe accurately how PCP variability functions in this region. Further south, there is also a positive SSRD-cPCP correlation, but it will not be assessed here since, as shown in the PCP climatologies, that region usually has little precipitation. On the other hand, sPCP-SSRD correlation is negative throughout the tropical Pacific, including the eastern ITCZ, and does not have any significant positive correlations. After examining these correlations, we observe that the eastern ITCZ suggests a new PCP scheme where precipitation is separated into convective and stratiform components:

$$sPCP : \uparrow sPCP \Rightarrow \downarrow SSRD \Rightarrow \downarrow SST$$

$$cPCP : \uparrow cPCP \Rightarrow \uparrow SSRD \Rightarrow \uparrow SST$$

While the sPCP scheme in the eastern ITCZ is equal to the Atm-driven mechanism, cPCP there is positively correlated with both SST and SSRD, which does not correspond to any of the PCP mechanisms considered.

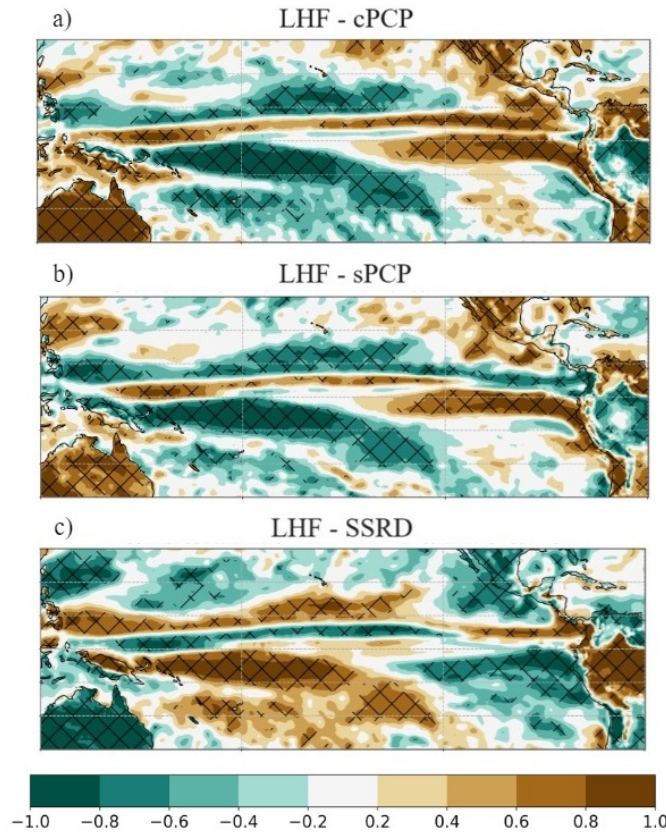


Figure 5. a), b) and c): Correlation coefficient between model surface LHF and model cPCP, sPCP and SSRD respectively. LHF is defined positive upwards and SSRD is defined positive downwards. Statistically significant regions at 95% confidence level are hatched.

A more complex analysis is needed to understand this behaviour. The first step is to examine the correlation between cPCP and sPCP, shown in Fig 4c. Stratiform and convective precipitation are positively correlated throughout the tropical Pacific, indicating that their variability tends to be synchronous. However, they are negatively correlated in the eastern ITCZ. This negative correlation suggests that when one component shows a negative anomaly (e.g., a decrease in sPCP), the other one shows a positive anomaly (e.g., an increase in cPCP).

To further understand this contrasting behaviour of cPCP and sPCP in the eastern ITCZ, we need to consider the role of LHF influencing precipitation patterns. LHF, which represents the energy transferred from the ocean to the atmosphere due to evaporation, is defined positive upwards. Figs 5a and 5b show the correlation coefficient of LHF-cPCP and LHF-sPCP respectively. In the eastern ITCZ, correlation between LHF and cPCP is predominantly positive. This suggests a strong ocean-atmosphere interaction: higher SST leads to increased evaporation and therefore increased LHF. Subsequently,

there is an increase in cPCP driven by this initial SST anomalies. On the other hand, correlation between LHF and sPCP in the eastern ITCZ is generally negative indicating that increased latent heat flux is associated with decreased stratiform precipitation. This negative correlation could suggest that when more energy is transferred from the ocean to the atmosphere through evaporation, the conditions become more favourable for convective processes and stratiform precipitation decreases, consistent with the negative correlation between cPCP-sPCP (Fig 4c). Fig 5c shows the correlation coefficient of LHF and SSRD. SSRD is defined positive downwards, while LHF is defined positive upwards. Therefore, correlations can be interpreted similarly to those with scalar fields: positive correlation between these two fluxes indicates simultaneous increase or decrease in their respective directions, while negative correlation indicate that an increase in one flux is associated with a decrease in the other. A positive LHF-SSRD correlation is observed over the eastern ITCZ. These result helps closing the correlation scheme between cPCP and sPCP in the eastern ITCZ: decrease (increase) in sPCP is associated with an increase (decrease) of SSRD which leads to an increase (decrease) in SST, hence an increase (decrease) in LHF which then increases (decreases) cPCP. A scheme for this mechanism is presented in Fig 6.

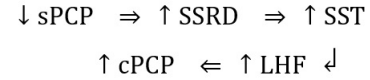


Figure 6. PCP scheme for the eastern ITCZ

Additionally, LHF correlation maps (Fig. 5) suggest much more about PCP variability. In the western-central Pacific, correlation dipoles appear in the ITCZ region for both cPCP-LHF and sPCP-LHF. These dipoles suggest a complex interaction between LHF and precipitation patterns, probably influenced by ENSO. During El Niño events, anomalous warming in the central and eastern Pacific trigger shifts in the ITCZ, altering precipitation patterns in this region. The positive correlation areas in these dipoles, at the equatorward flank, could represent regions where increased SST and associated LHF enhance both cPCP and sPCP, aligning with the warm phase of ENSO. Conversely, the negative correlation areas, at the poleward flank, might indicate regions where the usual precipitation patterns are disrupted, due to this ITCZ latitudinal shift. In the eastern ITCZ, a dipole is observed for sPCP, also suggesting a potential shift of precipitation towards the equator during El Niño events. This potential shift might contribute to decrease (increase) cloudiness in the eastern ITCZ and influence the SSRD, leading to increased (decreased) cPCP as discussed above. The absence of an LHF-cPCP correlation dipole in the eastern ITCZ further strengthens this idea.

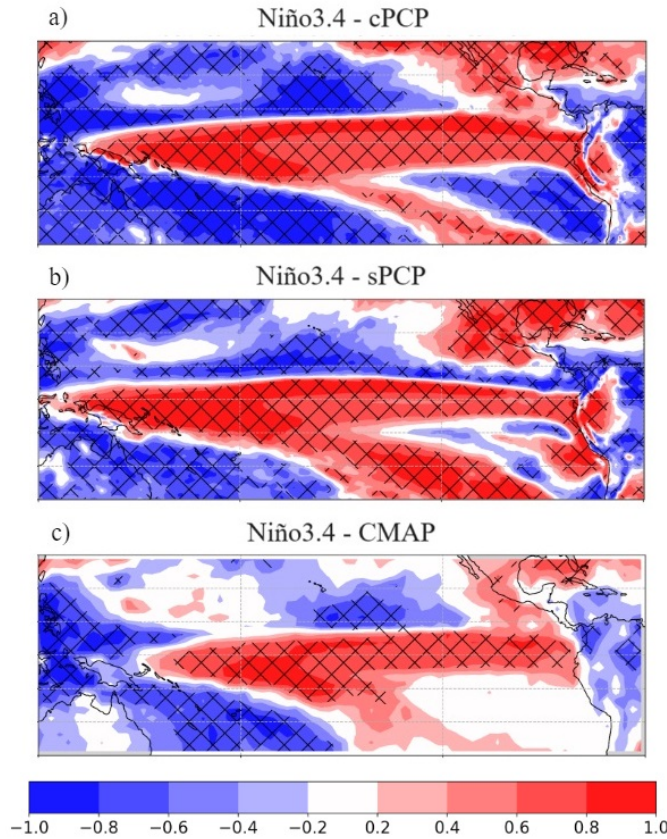


Figure 7. a), b) and c): Correlation coefficient between model Niño-3.4 index and model cPCP, model sPCP, and CMAP precipitation reanalysis respectively. Statistically significant regions at 95% confidence level are hatched.

To further explore The ENSO effect on precipitation, the Niño-3.4 index is analysed. As mentioned in the Introduction, ENSO variability is well represented with this index, so correlations between other variables and Niño-3.4 are no longer point-to-point, but connected to ENSO variability. Figs 7a, 7b, and 7c show the correlation coefficients between Niño-3.4 and cPCP, sPCP, and CMAP total precipitation, respectively. Positive (negative) correlations indicate an increase (decrease) of precipitation during a positive ENSO phase (El Niño). Positive correlations in the central and eastern Pacific and negative correlations in the western Pacific are observed for all three maps. For both sPCP and cPCP, a correlation dipole is observed at the western-central ITCZ region, indicating a decrease in precipitation north of the climatological ITCZ and an increase towards the equator during El Niño events. A dipole in the eastern ITCZ is observed only in sPCP, reinforcing our earlier finding of the latitudinal shift of stratiform precipitation towards the equator during El Niño. On the other hand, cPCP is positively correlated in this region, indicating that convective precipitation increases not only at the

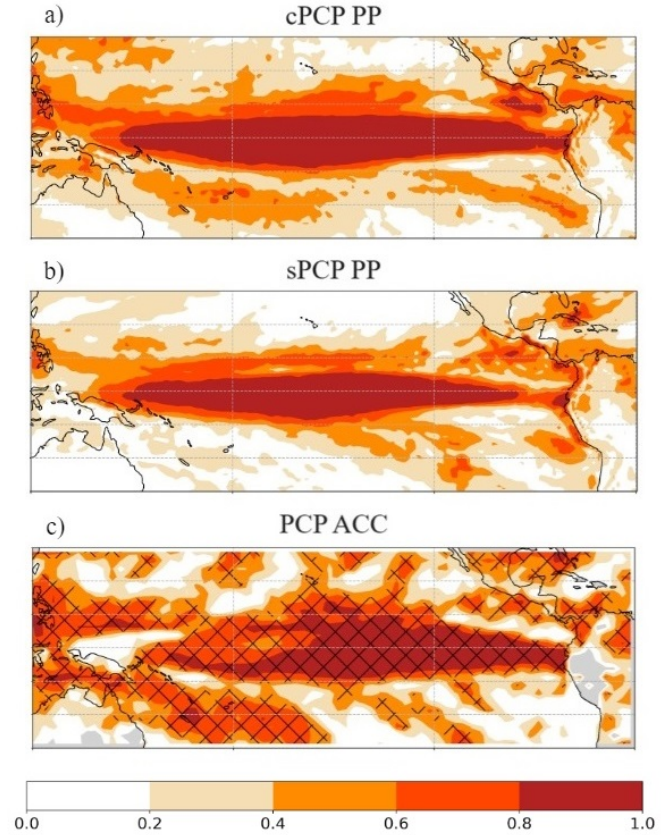


Figure 8. a) and b): Model cPCP and sPCP potential predictability. c) Correlation coefficient between observed and simulated total precipitation. Model total precipitation is considered as the sum of cPCP and sPCP. Statistically significant regions at 95% confidence level are hatched.

equator but also in the eastern ITCZ. This pattern is consistent with the LHF correlations, in Figs 5a and 5b, where warmer SSTs lead to enhanced convective activity rather than stratiform precipitation. The CMAP correlation map with the Niño-3.4 index resemble those in the model, with positive correlations in the central and eastern Pacific and negative correlations in the western Pacific. This map confirms that total precipitation during El Niño events generally increases in the central and eastern equatorial Pacific, and decreases further north. However, it is important to note that the correlation pattern in CMAP is not exactly the same as those in the cPCP and sPCP correlation maps. For example, the eastern ITCZ or the SST cold tongue do not have much correlation with ENSO according to Fig 7c. These discrepancies might be caused because we are comparing the total precipitation of the reanalysis with model cPCP and sPCP. The mixed variability these two components have, could lead to the differences observed in the total precipitation of the reanalysis.

Climate models have made significant progress in simulating precipitation patterns by separately identifying cPCP and sPCP. This separation allows models to capture their distinct responses to climatic drivers such as ENSO. However, when assessing model performance, the focus is typically on total precipitation, which may present significant challenges due to the mixed variability of cPCP and sPCP, as we just discussed. So, before dealing with model total PCP skill, we can evaluate the potential predictability of cPCP and sPCP individually. Figs 8a and 8b show cPCP and sPCP potential predictability respectively. Fig 8c depicts the skill of the EC-EARTH hindcasts in predicting total precipitation, using CMAP as reference. cPCP and sPCP potential predictability maps are quite similar. It is observed in both a large potential predictability throughout all the equatorial Pacific. The western-central ITCZ region does also have high potential predictability but it is lower in sPCP. However, where cPCP and sPCP differ the most is over the eastern ITCZ. In cPCP potential predictability we observe a large spot north of the eastern ITCZ connected to the equatorial region. In the sPCP map though, potential predictability there is lower. These cPCP and sPCP differences may explain why model skill, in Fig 8c, is practically zero in the eastern ITCZ region. The contrasting variability of the two PCP components in this area could result in their cancellation when considered together, leading to a bad model performance. Although the separation of PCP has been useful for studying and evaluating different climate patterns, maybe the model cannot translate their variability into PCP skill in the eastern ITCZ since it is not easy to separate observed precipitation into stratiform and convective precipitation.

IV. CONCLUSIONS

Exploring in detail convective and stratiform precipitation in the tropical Pacific has allowed us to see their distinct mechanisms and responses to climate variability. We conclude that cPCP is primarily driven by SST, with warmer SSTs leading to increased convective activity and, on the other hand, sPCP can be more influenced by atmospheric processes. This difference is particularly evident in the target region of the study, the eastern ITCZ. There, sPCP variability is opposite to cPCP. Thanks to the study of LHF correlation with both PCP components, we can conclude that LHF substantially contributes to increase cPCP rather than sPCP, explaining the negative correlation between them in the eastern ITCZ. Additionally, both types of precipitation have a strong correlation with LHF and ENSO variability which are mainly the ones responsible for PCP variability there. These correlations also display a dipole pattern caused by El Niño events, where increased precipitation occurs towards the equator and decreased precipitation is found north of the climatological ITCZ. In the eastern ITCZ though, it is possible for convective

precipitation to increase when the ITCZ is shifted to the equator, and therefore no dipole is observed for cPCP.

Our study also claims for the need to distinguish between the different types of precipitation in observational data, if at all possible. This is thought to be responsible for limiting the accuracy of model skill. For example, in the eastern ITCZ, the contrasting variability of cPCP and sPCP can cancel each other, leading to no prediction skill for total precipitation. Understanding the dynamics and responses of convective and stratiform PCP has been essential to understand climate modelling in the tropical Pacific region. This insight has enhanced our understanding of the precipitation predictions formulated by the model.

However, we would like to remark that our analysis is based on a seasonal-mean scale. To improve this study, separating data into different months instead of considering a seasonal mean could help improving the time characteristics of the correlations. With this approach, it would be possible to better understand the regions where sPCP and cPCP were negatively correlated. For example, knowing which one decreases or increases first or if their variability is cancelling during the whole season or intra-seasonally can help understanding PCP skill each month. Also, with this monthly analysis, a time lag correlation could be made between PCP, SSRD and LHF to confirm the causality of the PCP schemes we have considered. Finally, we should also consider that some of the results discussed here are model dependent. So, a multi-model analysis could be another way forward to improve the analysis.

ACKNOWLEDGMENTS

I would like to thank Javi and Yolanda for their support and guidance throughout this study, and my family and friends for their love, patience, and support.

REFERENCES

- Arakawa, O. and A. Kito, 2004: Comparison of local precipitation-SST relationship between the observations and a reanalysis data-set. *Geophysical Research Letters*, *31*, L12206.
- Bjerknes, J., 1969: Atmospheric teleconnections from the equatorial Pacific. *Monthly Weather Review*, *97*(3), 163–172.
- Buizza, R., et al., 1999: Stochastic representation of model uncertainties in the ECMWF ensemble prediction system. *Quarterly Journal of the Royal Meteorological Society*, *125*, 2887–2908.

- Chen, M., W. Wang, and A. Kumar, 2012: Ocean surface impacts on the seasonal-mean precipitation over the tropical Indian Ocean. *Journal of Climate*, *25*, 3566-3582.
- Deser, C., M. A. Alexander, S.-P. Xie, and A. S. Phillips, 2010: Sea surface temperature variability: Patterns and mechanisms, *Annual review of marine science*, (2), 115-143.
- ECMWF IFS Documentation CY41R2, 2016: Part IV, Physical Processes: Chapters 6 and 7.
- Haarsma, R.J., García-Serrano, J., Prodhomme, C. et al., 2019: Sensitivity of winter North Atlantic-European climate to resolved atmosphere and ocean dynamics. *Scientific reports* *9*, 13358.
- Holloway, C., and J. D. Neelin, 2009: Moisture Vertical Structure, Column Water Vapor, and Tropical Deep Convection. *Journal of the Atmospheric Sciences*, *66*, 1665-1683.
- Johnson, N., S.-P. Xie, 2010: Changes in the sea surface temperature threshold for tropical convection. *Nature Geoscience* *3*, 842-845.
- Kumar, A., M. Chen, and W. Wang, 2013: Understanding Prediction Skill of Seasonal Mean Precipitation over the Tropics. *Journal of Climate*, *26*, 5674-5681.
- Prodhomme, C., et al., 2016: Benefits of Increasing the Model Resolution for the Seasonal Forecast Quality in EC-Earth. *Journal of Climate*, *29*, 9141-9162,
- Tapiador, F., et al., 2012: Global precipitation measurement: Methods, datasets and applications. *Atmospheric Research*, *104-105*, 70-97.
- Waliser, D., and N. E. Graham, 1993: Convective cloud systems and warm-pool sea surface temperatures: Coupled interactions and self-regulation. *Journal of Geophysical Research*, *98(D7)*, 12881-12893.
- Wallace, J., and Hobbs, P., 2006: Atmospheric Science: An Introductory Survey. *Chapters 4 & 6*.
- Wang, C., and J. Picaut, 2004: Understanding ENSO physics-a review. *Geophysical Monograph Series*, *147*, 21-48.
- Xie, S.-P., 2004: The shape of continents, air-sea interaction and the rising branch of the Hadley circulation. *The Hadley Circulation: Past, Present and Future*, *Kluwer Academic Publishers*, 121-152.